Predicting monomers for use in polymerization-induced self-assembly

Foster, Jeffrey; Varlas, Spyridon; Couturaud, Benoit; Jones, Joseph Rueben; Keogh, Robert; Mathers, Robert T.; O'Reilly, Rachel K.

DOI:
10.1002/anie.201809614

Predicting Monomers for use in Polymerization Induced Self-Assembly

Jeffrey C. Foster,[a] Spyridon Varlas,†[a] Benoit Couturaud,†[a] Joseph R. Jones,[a] Robert Keogh,[b] Robert T. Mathers,*[c] and Rachel K. O'Reilly*[a]

Abstract: We report an *in silico* method to predict monomers suitable for use in polymerization-induced self-assembly (PISA). By calculating the dependence of $LogP_{oct}$/surface area (SA) on the length of the growing polymer chain, the change in hydrophobicity during polymerization was determined. This allowed for evaluation of the capability of a monomer to polymerize to form self-assembled structures during chain extension. Using this method, we identified five new monomers for use in aqueous PISA *via* reversible addition-fragmentation chain transfer (RAFT) polymerization, and confirmed that these all successfully underwent PISA to produce nanostructures of various morphologies. The results obtained using this method correlated well with and predicted the differences in morphology obtained from the PISA of block copolymers of similar molecular weight but different chemical structures. Thus, we propose this method can be utilized for the discovery of new monomers for PISA and also the prediction of their self-assembly behavior.

Polymerization-induced self-assembly (PISA) has revolutionized the preparation of soft nanoparticles.[1] Unlike traditional self-assembly strategies, in which a block copolymer is synthesized separately and transitioned into aqueous milieu,[2] PISA occurs *in situ* as the polymerization progresses. During aqueous PISA, a water-soluble homopolymer is chain-extended with a second, water-miscible monomer.[3] As the polymerization proceeds, the second block becomes gradually insoluble in the reaction media, driving self-assembly.[4] A variety of self-assembled morphologies can be readily accessed by tuning polymerization conditions.[5] In addition to its simplicity, PISA is advantageous as it can be conducted at high solids content (typically 10-30 w/w%) to quantitative or near quantitative conversion of monomer.

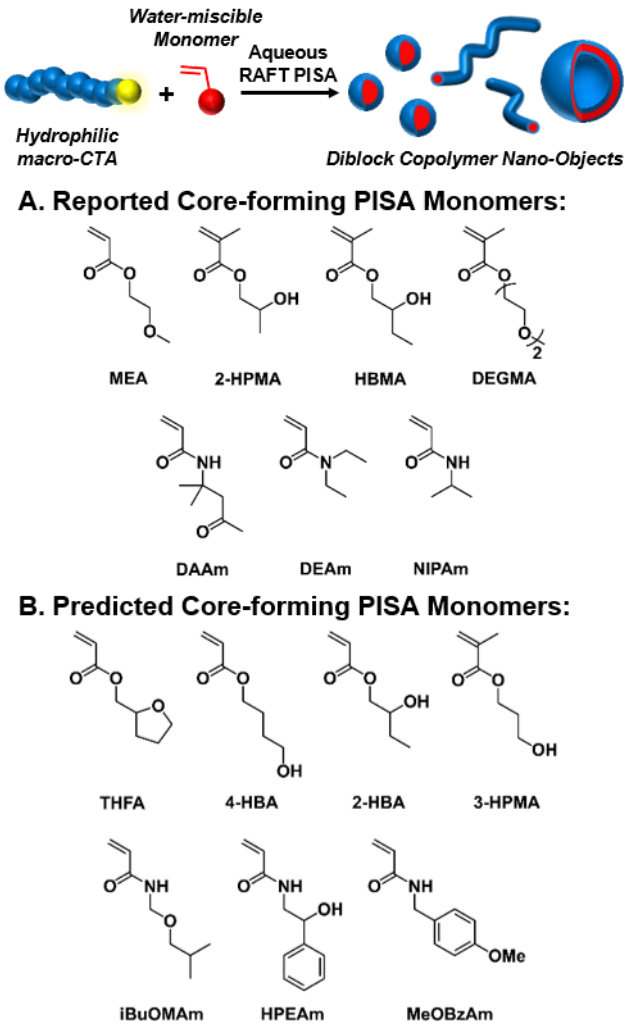

Figure 1. Schematic illustration of the aqueous RAFT PISA process, A) Core-forming monomers identified in the literature for use in RAFT PISA in aqueous milieu and B) predicted core-forming monomers.

Polymer nanoparticles obtained from PISA have applications in nanomedicine and drug delivery,[6] especially in the case of worm or vesicle morphologies, which have specific advantages over

[a] Dr. J. C. Foster, S. Varlas, Dr. B. Couturaud, Dr. J. R. Jones, Prof. R. K. O'Reilly
School of Chemistry, University of Birmingham
Edgbaston, Birmingham, B15 2TT (UK)
E-mail: r.oreilly@bham.ac.uk
[b] R. Keogh
Department of Chemistry, University of Warwick
Gibbet Hill Road, Coventry, CV4 7AL (UK)
[c] Prof. R. T. Mathers
Department of Chemistry, Pennsylvania State University
New Kensington, PA 15068 (USA)
E-mail: rtm11@psu.edu

Supporting information for this article is given via a link at the end of the document.

†These authors contributed equally to this work.

spherical micelles. In particular, these morphologies often have higher loading capacities than spherical micelles and different *in vivo* cell adsorption and internalization behavior.[7] In the case of polymeric vesicles, both hydrophobic and hydrophilic payloads can be encapsulated due to the fact that they possess both a vesicle membrane and an aqueous interior.[8]

In principle, PISA can be carried out using any type of controlled/living polymerization; however, the vast majority of examples in the literature concern the use of reversible addition-fragmentation chain transfer (RAFT) polymerization. RAFT is well-suited for PISA due to its wide monomer scope and tolerance towards most conventional reaction media including polar- and non-polar organic solvents, ionic liquids, and most importantly, water.[9] To date, a number of vinyl monomers have been identified that undergo PISA *via* RAFT in aqueous milieu (Figure 1A); for example, acrylates (MEA),[10] methacrylates (HPMA, HBMA, DEGMA),[5, 11] and acrylamides (DAAm, DEAm, NIPAM)[12] have all been utilized successfully. In light of the diversity of these monomer examples, there exists no clear principle to identify whether a certain monomer can be utilized to conduct PISA in a given solvent. Indeed, most of the monomers found to undergo PISA appear to have been identified empirically. In other words, the capability of a monomer to undergo PISA is most often recognized during polymerization, indicated by an onset of turbidity within the polymerization solution.

In this contribution, we report a generalized *in silico* method to predict whether a given monomer will undergo PISA in water. This method evaluates the variance in polymer hydrophobicity with increasing chain length, which is hypothesized to be a key feature in determining if the monomer is capable of behaving as a core-forming monomer for PISA. Application to monomers known to undergo PISA resulted in the emergence of a trend through which additional PISA monomers could be predicted. Then, this method was utilized to identify proposed new PISA monomers (Figure 1B). Validation of these new monomers *via* RAFT polymerization in water confirmed the capability of our method to predict new monomers for PISA.

The underlying methodology for predicting PISA behavior involves calculating the hydrophobicity of oligomeric models using octanol-water partition coefficients ($LogP_{oct}$). For several decades, this metric has served as a key predictor of drug solubility for the pharmaceutical industry.[13] Although it has only recently adapted for polymer science, the versatility of $LogP_{oct}$ values has facilitated assessment of condensation polymerizations,[14] UV-cured films,[15] post-polymerization modifications,[16] polymer electrolytes,[17] and crystallization-driven self-assembly (CDSA).[18] During initial efforts to switch the focus from small, drug-like molecules to larger polymeric structures, normalizing $LogP_{oct}$ values with surface area (SA) minimized end-group effects and molecular weight differences.[15]

When molecules experience a two-phase environment, such as octanol and water, positive $LogP_{oct}$ values indicate the molecule is hydrophobic and mostly partitions into the octanol phase. In contrast, negative $LogP_{oct}$ values confirm a preference for solubility in the aqueous phase. In Figure 2, four previously reported core-forming polymers (as shown in Figure 1A) were calculated to exhibit positive $LogP_{oct}$/SA values (for short oligomers, 6-mers) and positive slopes upon increasing the block length to 24. As a comparison, we performed the same calculation for three well-established water-soluble oligomers and polymers

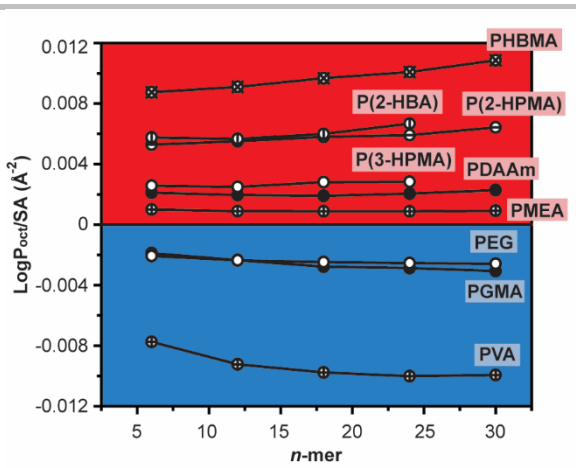

Figure 2. Evolution of oligomer hydrophobicity as a function of the length of the oligomer. $LogP_{oct}$ values (ALogP98 method) normalized by Connolly surface area (SA). Blue region indicates corona-forming blocks and red region indicates core-forming blocks in aqueous PISA.

and indeed they demonstrated an opposite trend. This analysis was further applied to a wide range of previously reported monomers, as shown in Figure S1. Based on this analysis, the magnitude of $LogP_{oct}$/SA and corresponding slope predicts whether a unimer will achieve increasing hydrophobicity during propagation and thus enable its utilization as a core-forming monomer in PISA. While the slope and magnitude in Figure 2 will be influenced by experimental parameters (i.e., temperature, solvent, and pH), computational predictions of hydrophobicity appear to accommodate a wide variety of functional groups found in polymer science. As such, the trends observed in $LogP_{oct}$/SA for neutral polymers at pH ~7 appear to be universal and provide an insight into the upper and lower limits of hydrophobicity for core-forming PISA monomers.

The magnitude of the $LogP_{oct}$/SA values shown in Figure 2 conveys meaningful insight into the overall hydrophobicity of the growing polymer chain. For example, oligomers prepared from 2-HPMA possess $LogP_{oct}$/SA values that are ca. 0.004 $Å^{-2}$ greater than those of MEA across all chain lengths. Because the hydrophobicity of the growing polymer chain affects its partitioning between water and organic phases, relative comparisons of the magnitude of $LogP_{oct}$/SA could potentially predict both the length of the chain required to induce micellization and the predominate morphology for a given oligomer length. We consider PEG-*b*-PHPMA and PEG-*b*-PMEA block copolymers reported by Armes and Meada, respectively.[19] For PEG_{113}-*b*-$PHPMA_{300}$, unimolecular vesicles are obtained at 10 wt% solids, while spherical micelles are reported for PEG_{113}-*b*-$PMEA_{300}$ at the same concentration. This difference in morphology between polymers of similar molecular weight can be rationalized in terms of their relative hydrophobicities. As our model predicts *via* the magnitude of the LogPoct/SA value, polymers of 2-HPMA are more hydrophobic than those of MEA. Thus, higher-order morphologies are obtained for 2-HPMA than for MEA at the same degree of polymerization (DP) and concentration.

Using our predictive model, seven further vinyl monomers were selected based on either their commercial availability or their

similarity to monomers that have been previously reported to undergo PISA (Figure 1B). For example, THFA and *i*BuOMAm can be purchased from commercial vendors, while 3-HPMA is a structural isomer of 2-HPMA. 2-HPMA is perhaps the most commonly utilized core-forming monomer in PISA, which is most often obtained as a mixture of isomers. Because the $LogP_{oct}$/SA values of 3-HPMA are less than those of 2-HPMA by almost a factor of two, the behavior of commercial isomeric monomer mixtures during PISA is expected to depend on their respective molar ratios. We also chose to compare the $LogP_{oct}$/SA values and self-assembly behavior of 4-HBA and 2-HBA, another pair of structural isomers. These monomer pairs would, we envisioned, yield meaningful insight into structure/hydrophobicity relationships. Toward this end, $LogP_{oct}$/SA values were calculated for these monomers at various oligomer lengths as shown in Figure 2 and Figure S1.

Interestingly, all seven of the predicted monomers were found to reside in the hydrophobic region of the $LogP_{oct}$/SA *vs* n-mer plot shown in Figure 2 and Figure S1 and possessed positive slopes. This suggested that all of the monomers shown in Figure 1B were predicted to be suitable as core-forming monomers in PISA. It should be noted that the acrylamides HPEAm and MeOBzAm were solids at room temperature and could not be dissolved in H_2O at concentrations relevant for PISA (i.e., ≥ 10 wt%). Therefore, this approach for identifying potential PISA monomers is limited by the fact that it does not give direct information about the solubility of the monomer itself in H_2O. The remaining five monomers each appeared to be miscible with H_2O at concentrations as high as 25 wt%.

We then evaluated the capability of the five water-miscible monomers—3-HPMA, 4-HBA, THFA, 2-HBA, and *i*BuOMAm—to undergo PISA in aqueous media. A series of polymerizations were carried out for these monomers *via* RAFT using a PEGylated chain transfer agent (macro-CTA, M_n ~ 5 kDa). For these experiments, the concentration of monomer was held constant at 25 w/w%, the [macro-CTA]/[initiator] ratio was maintained at 1 : 0.1, and the [monomer]/[macro-CTA] ratio was varied to target different degrees of polymerization. The polymerizations were initiated using 2,2'-azobis(2-methylpropionamidine)dihydrochloride (V-50), which is water-soluble, and were heated at 50 °C for 2-6 h until the monomer conversions had reached ≥ 90%. The polymerization samples were then analyzed by size-exclusion chromatography (SEC) and transmission electron microscopy (TEM).

In all cases, RAFT PISA using the five monomers resulted in the formation of self-assembled morphologies, regardless of the targeted DP. Molecular weight distributions were generally narrow, with experimentally measured MWs that agreed well with expected values. PISA using THFA is highlighted in Figure 3. As shown in Figure 3B, RAFT polymerization followed pseudo-first-order kinetics, with a change in rate at ca. 10 min that corresponded to the onset of self-assembly. MW values increased linearly with increasing targeted DP (Figure 3B, inset), and dispersity values remained low for the polymerizations targeting DPs of 50, 75, and 100 ($Đ_M$ ≤ 1.3), but was higher for the DP 200 sample ($Đ_M$ = 1.56). In addition, the self-assembled morphologies evolved from worms to a mixed morphology containing worms and vesicles to pure vesicles as the DP of the core block increased from 75 to 100 to 200, respectively (Figures 3D-3F). These morphologies were further confirmed using static

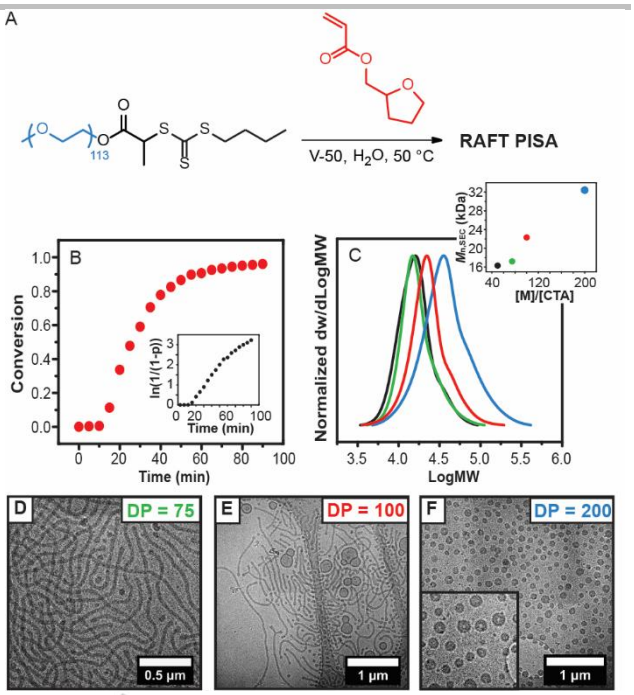

Figure 3. Evaluation of RAFT PISA using THFA as a core-forming block. A) Schematic of THFA aqueous PISA. B) Kinetic plots of polymerization targeting DP = 100. The inset shows the semilogarithmic plot. C) SEC RI traces of four different polymerizations targeting DPs of 50 (black trace and circle), 75 (green trace and circle), 100 (red trace and circle), and 200 (blue trace and circle). The inset shows the variance in M_n with DP. D-F) Cryo-TEM images after polymerization showing the evolution of morphology upon increasing DP. The size of the inset of F is 1 µm^2.

light scattering (SLS) by comparison with a theoretical form factor for disperse random coils in the case of the DP=75 sample and from a measured R_g/R_h ratio of 0.995 for the DP=200 sample which is consistent with hollow spheroids (Figure S22). Similar trends were observed for the other new monomers (SEC traces found in Figures S8-S10; TEM images in Figures S11-S15); however, a significant difference in the morphology of the self-assemblies was observed that depended on the monomer utilized, implying a correlation between the chemical nature of the monomer and the morphology of the resulting nanoparticles. It should be noted that some of the monomers utilized (THFA, 2- and 4-HBA) produced polymers with T_g values below room temperature. As such, the morphologies present immediately following polymerization may not be directly reflected by TEM images or SLS data, which are conducted at lower temperatures. The success of our evaluation of PISAs using the five predicted monomers validated prediction of new core-forming monomers using $LogP_{oct}$/SA calculations. In addition to predictive data, we wondered whether this quantitative treatment, which gives information about the relative hydrophobicity of polymer microstructures, could be correlated to other aspects of PISA. It is well understood that assembly morphology depends on factors such as the degree of stretching of the core-forming chains, the interfacial tension between the hydrophobic cores and their external environment, and repulsion between corona chains.[2] These parameters are most often tuned by varying the relative volume fraction of the hydrophobic and hydrophilic blocks.[20] In contrast, there has been little study into how the chemistry of the

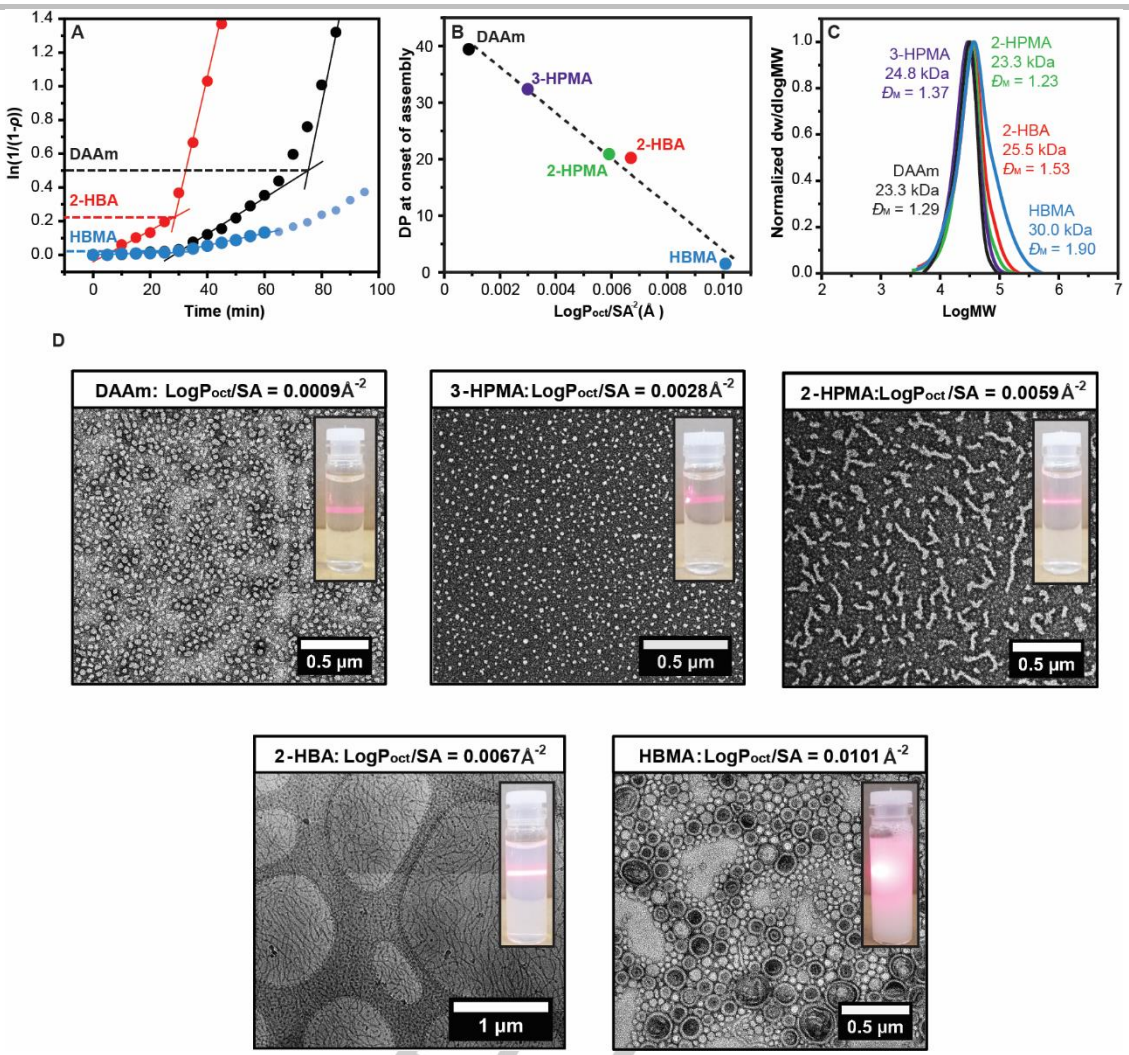

Figure 4. Morphological prediction and rationalization using $LogP_{oct}/SA$ method. A) Semi-logarithmic kinetic plots for RAFT PISA using DAAm, 2-HBA, and HBMA targeting DP = 100. B) Plot of the DP at the onset of assembly as a function of $LogP_{oct}/SA$. C) SEC RI traces of the RAFT PISAs using DAAm, 3-HPMA, 2-HPMA, 2-HBA, and HBMA. D) Dry-state (DAAm, 3-HPMA, 2-HPMA, and HBMA) or cryo-TEM (2-HBA) images of RAFT PISAs using these five monomers after polymerization. The insets show an increase in turbidity of the polymerization solutions with increasing polymer hydrophobicity.

core-forming chains affects self-assembly. As the interfacial tension between the cores of the self-assembled aggregates and their solvent environment depends principally on the hydrophobicity of the polymer chains located at that interface, we envisioned that our $LogP_{oct}/SA$ analysis could enable morphological prediction. Therefore, we hypothesized that for block copolymers with identical corona and core block lengths, changes in $LogP_{oct}/SA$ of the hydrophobic block could be related to the morphology of the self-assembled particles.

To evaluate this hypothesis, we conducted five polymerizations using DAAm, 3-HPMA, 2-HPMA, 2-HBA, and HBMA under otherwise identical experimental conditions. Separate polymerizations were conducted targeting DP = 100 in the hydrophobic block using each monomer. Our analysis of polymerization kinetics, as well as SEC traces of the resulting block copolymers and TEM images of the nanoparticles after polymerization are summarized in Figure 4.

For PISA, a change in slope is expected in the semi-logarithmic plot which corresponds to the onset of assembly. This inflection originates as sequestration of monomer within the cores of the assemblies accelerates polymerization rate, leading to high local monomer concentration. Indeed, these transitions are apparent in Figure 4A (additional kinetic data provided in Figures S17-S21), with the onset of assembly dependent upon the monomer utilized. A plot of the DP of the core block at which the onset of self-assembly occurred *vs* the $LogP_{oct}/SA$ value of the oligomeric species of the corresponding polymer yielded a linear relationship. Unsurprisingly, the length of the core-forming block required to induce self-assembly decreased with increasing oligomer hydrophobicity. More significantly, the morphologies of the resulting assemblies, which arose *via* self-assembly of block copolymers of approximately equal molecular weight (Figure 4C) also varied dramatically with $LogP_{oct}/SA$. As shown in Figure 4D, the least hydrophobic polymers prepared from DAAm and 3-HPMA, self-assembled into small, spherical micelles. 2-HPMA and 2-HBA, forming polymers of intermediate hydrophobicity, produced worm-like micelles. Finally, the most hydrophobic polymers, formed of HBMA, produced a mixed morphology which contained worm-like micelles and polymeric vesicles.

In summary, we report an *in silico* method that predicts monomers that can be utilized in aqueous PISA. By calculating the variance in $LogP_{oct}$/SA with increasing oligomer length, the change in hydrophobicity can be evaluated and related to the capability of the monomer to form self-assembled structures during polymerization. Using this method, we identified five new monomers for use in RAFT PISA, and these were found to successfully undergo PISA to produce various nano-object morphologies such as spheres, worms, and vesicles. Interestingly, this method was also leveraged to gain insight into both the onset of self-assembly during PISA and the resulting morphology. As the hydrophobicity of the monomers and their oligomers increased, the onset of assembly occurred at lower DPs. Additionally, when comparing block copolymers of approximately the same length, monomers that produced oligomers with higher $LogP_{oct}$/SA values resulted in higher-order assemblies. We anticipate that this model will evaluate suitability of given monomer for PISA. Since novel monomers are often designed with specific functionality in mind, our general method should provide information about their polymerization-dependent solubility while giving predictive insight into the morphology of the self-assembled structures that result from PISA.

Acknowledgements

This work was supported by the ERC (615142). B. Couturaud acknowledges funding from the European Union's Horizon 2020 research and innovation programme under the Marie Sklodowska-Curie grant agreement No 703934, FluoroDendriNostic project. Advanced BioImaging Research Technology Platform, BBSRC ALERT14 award BB/M01228X/1 is thanked for supporting cryo-TEM analysis, and Dr. S. Bakker, University of Warwick, is thanked for assistance.

Keywords: PISA, RAFT polymerization, nanoparticles, structure-property relationships, polymer hydrophobicity

[1] a) N. J. Warren, S. P. Armes, *J. Am. Chem. Soc.* **2014**, *136*, 10174-10185; b) B. Charleux, G. Delaittre, J. Rieger, F. D'Agosto, *Macromolecules* **2012**, *45*, 6753-6765; c) J.-T. Sun, C.-Y. Hong, C.-Y. Pan, *Polym. Chem.* **2013**, *4*, 873-881.

[2] Y. Mai, A. Eisenberg, *Chem. Soc. Rev.* **2012**, *41*, 5969-5985.

[3] a) S. L. Canning, G. N. Smith, S. P. Armes, *Macromolecules* **2016**, *49*, 1985-2001; b) J. Rieger, F. Stoffelbach, C. Bui, D. Alaimo, C. Jérôme, B. Charleux, *Macromolecules* **2008**, *41*, 4065-4068.

[4] A. Blanazs, A. J. Ryan, S. P. Armes, *Macromolecules* **2012**, *45*, 5099-5107.

[5] J. Rieger, *Macromol. Rapid Commun.* **2015**, *36*, 1458-1471.

[6] L. D. Blackman, S. Varlas, M. C. Arno, Z. H. Houston, N. L. Fletcher, K. J. Thurecht, M. Hasan, M. I. Gibson, R. K. O'Reilly, *ACS Cent. Sci.* **2018**, *4*, 718-723.

[7] a) T. Li, H. Walter, L. Yaling, H. Gang, D. S. Baran, G. Jinming, *Exp. Bio. Med.* **2011**, *236*, 20-29; b) S. E. A. Gratton, P. A. Ropp, P. D. Pohlhaus, J. C. Luft, V. J. Madden, M. E. Napier, J. M. DeSimone, *PNAS* **2008**, *105*, 11613.

[8] P. Tanner, P. Baumann, R. Enea, O. Onaca, C. Palivan, W. Meier, *Acc. Chem. Res.* **2011**, *44*, 1039-1049.

[9] D. J. Keddie, *Chem. Soc. Rev.* **2014**, *43*, 496-505.

[10] S. Sugihara, A. H. Ma'Radzi, S. Ida, S. Irie, T. Kikukawa, Y. Maeda, *Polymer* **2015**, *76*, 17-24.

[11] a) Y. Li, S. P. Armes, *Angew. Chemie. Int. Ed.* **2010**, *49*, 4042-4046; b) J. Tan, H. Sun, M. Yu, B. S. Sumerlin, L. Zhang, *ACS Macro Lett.* **2015**, *4*, 1249-1253; c) L. P. D. Ratcliffe, A. Blanazs, C. N. Williams, S. L. Brown, S. P. Armes, *Polym. Chem.* **2014**, *5*, 3643-3655.

[12] a) X. Wang, C. A. Figg, X. Lv, Y. Yang, B. S. Sumerlin, Z. An, *ACS Macro Lett.* **2017**, *6*, 337-342; b) M. J. Derry, L. A. Fielding, S. P. Armes, *Prog. Polym. Sci.* **2016**, *52*, 1-18; c) C. A. Figg, A. Simula, K. A. Gebre, B. S. Tucker, D. M. Haddleton, B. S. Sumerlin, *Chem. Sci.* **2015**, *6*, 1230-1236.

[13] a) C. A. Lipinski, F. Lombardo, B. W. Dominy, P. J. Feeney, *Adv. Drug Deliv. Rev.* **1997**, *23*, 3-25; b) A. A. Petrauskas, E. A. Kolovanov, *J. Comput. Aided Mol. Des.* **2000**, *19*, 99-116; c) A. K. Ghose, V. N. Viswanadhan, J. J. Wendoloski, *J. Phys. Chem. A.* **1998**, *102*, 3762-3772.

[14] a) D. Dakshinamoorthy, A. K. Weinstock, K. Damodaran, D. F. Iwig, R. T. Mathers, *Chem. Sus. Chem.* **2014**, *7*, 2923-2929; b) A. G. Soxman, J. M. DeLuca, K. M. Kinlough, D. F. Iwig, R. T. Mathers, *J. Poly. Sci. Part A: Polym. Chem.* **2017**, *55*, 3308-3316.

[15] A. J. D. Magenau, J. A. Richards, M. A. Pasquinelli, D. A. Savin, R. T. Mathers, *Macromolecules* **2015**, *48*, 7230-7236.

[16] J. Waggel, R. T. Mathers, *RSC Adv.* **2016**, *6*, 62884-62889.

[17] E. Yildirim, D. Dakshinamoorthy, M. J. Peretic, M. A. Pasquinelli, R. T. Mathers, *Macromolecules* **2016**, *49*, 7868-7876.

[18] M. Inam, G. Cambridge, A. Pitto-Barry, Z. P. L. Laker, N. R. Wilson, R. T. Mathers, A. P. Dove, R. K. O'Reilly, *Chem. Sci.* **2017**, *8*, 4223-4230.

[19] a) N. J. Warren, O. O. Mykhaylyk, D. Mahmood, A. J. Ryan, S. P. Armes, *J. Am. Chem. Soc* **2014**, *136*, 1023-1033; b) S. Sugihara, A. H. Ma'Radzi, S. Ida, S. Irie, T. Kikukawa, Y. Maeda, *Polymer* **2015**, *76*, 17-24.

[20] S. Jain, F. S. Bates, *Science* **2003**, *300*, 460.

COMMUNICATION

We report a method to predict monomers suitable for use in PISA, which calculates the dependence of $LogP_{oct}$/SA on the length of the growing polymer chain. Using this method, we identified five new monomers for use in aqueous PISA *via* RAFT polymerization, and confirmed that they all successfully underwent PISA to produce nanostructures of various morphologies. Our method also explains trends observed between polymer hydrophobicity and its self-assembled morphology.

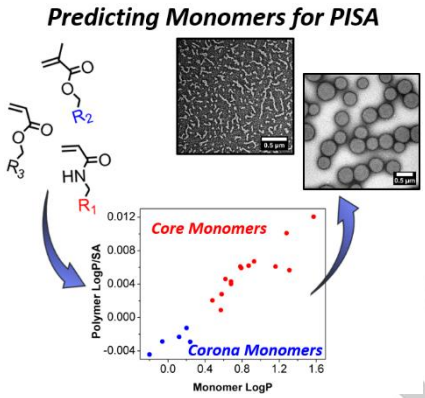

Jeffrey C. Foster,[a] Spyridon Varlas,†[a] Benoit Couturaud,† [a] Joseph R. Jones, [a] Robert Keogh,[b] Robert T. Mathers,[c] and Rachel K. O'Reilly*[a]*

Page No. – Page No.

Predicting Monomers for use in Polymerization Induced Self-Assembly